86. Structures and Electrical Properties of Some New Organic Conductors Derived from the Donor Molecule TMET (*S,S,S,S*-Bis(dimethylethylenedithio)tetrathiafulvalene)

by **Andreas Karrer, John D. Wallis,** and **Jack D. Dunitz***
Laboratorium für Organische Chemie, ETH-Zentrum, CH-8092 Zürich
and **Bruno Hilti*, Carl W. Mayer, Markus Bürkle,** and **Jürgen Pfeiffer**
Zentrale Forschung, *Ciba-Geigy AG*, CH-4002 Basel

(31.III.87)

Crystal structures and electrical properties of radical-cation salts of the chiral organic donor TMET (*S,S,S,S*-bis-(dimethylethylenedithio)tetrathiafulvalene) are described. Two structural types, 2:1 with octahedral anions PF_6^-, AsF_6^-, SbF_6^-, I_3^- (incommensurate), and 3:2 with tetrahedral anions BF_4^-, ClO_4^-, ReO_4^- are observed. Resistivity measurements between 2 and 298 K indicate that the 3:2 types are organic metals, while the other compounds are semiconductors. $(TMET)_3(ClO_4)_2$ is metallic down to about 120 K at ambient pressure and remains metallic down to 2 K at 8 kbar.

Introduction. – The donor molecule bis(ethylenedithio)tetrathiafulvalene (often abbreviated to BEDT-TTF or more simply ET) forms a variety of 2:1 salts, $(ET)_2X$ (X = monovalent anion), which span a wide range of structural types and physical properties [1]. Of special interest is the β-phase of $(ET)_2I_3$, which occurs in two slightly different modifications, both of which are superconducting, one below 1.5 K [2] and the other below 8 K [3]. This has led to intense activity in two directions: replacing I_3^- by other linear anions such as $AuBr_2^-$ and I_2Br^-, and introducing small structural changes in the donor [4].

We recently announced the synthesis of a chiral tetramethyl derivative of ET (TMET for short), and described the structure of a semiconducting 2:1 salt with PF_6^- as counterion [5]. We now describe the crystal structures and electrical properties of some further, highly conducting 2:1 salts with the counterions AsF_6^-, SbF_6^- and I_3^- (2:0.71), as well as of new organic metals of 3:2 stoichiometry formed with ClO_4^-, ReO_4^-, and BF_4^-.

Crystal Structures of $(TMET)_nX$ Salts. – X-Ray diffraction measurements have been made for crystalline salts of TMET with the anions listed in *Table 1*. All crystals examined

Table 1. *Room-Temperature Cell Constants and Approximate Stoichiometry of Seven TMET Salts.* Standard deviations (in parentheses) apply to the least significant digit; values without e.s.d.'s are taken from precession photographs. Z_D (Z_A) is the number of TMET molecules (anions) per unit cell.

Anion	a [Å]	b [Å]	c [Å]	α [°]	β [°]	γ [°]	V [Å^3]	Z_D	Z_A
PF_6^-	6.915(1)	8.085(3)	19.934(8)	90.64(3)	75.41(2)	70.98(2)	1014	2	1
AsF_6^-	6.94	8.10	19.93	90.02	74.7	71.1	≈ 1018	2	1
SbF_6^-	6.9	8.1	20.0	91	74	71	≈ 1009	2	1
I_3^-	6.85	8.01	19.68	95.4	87.7	72.6	≈ 1023	2	0.71
BF_4^-	6.872(2)	12.926(4)	20.168(4)	76.50(2)	76.53(2)	68.85(3)	1602	3	≈ 2
ClO_4^-	6.854(4)	12.951(4)	20.017(6)	76.77(3)	76.57(5)	68.75(5)	1590	3	≈ 2
at 200 K	6.825(7)	12.827(5)	19.955(9)	76.62(4)	76.50(7)	68.95(7)	1564	3	≈ 2
ReO_4^-	6.9	12.9	20.2	77	77	68.5	≈ 1619	3	≈ 2

belong to space group $P\bar{1}$ but show markedly pseudo-centrosymmetric features in their diffraction patterns. They may be divided into two structural types, as indicated in *Table 1*, and we shall refer to these as the 2:1 and 3:2 types, even though there is some uncertainty with respect to the exact compositions.

Crystals of all TMET salts obtained so far form black parallelepipeds bounded by the (100), (010), (001) faces and their opposites. Twinning across (100) or ($\bar{1}$00) is frequent. The longest crystal dimension is always along [010], the stacking direction, and the shortest is along [001]. Some $(TMET)_3(ClO_4)_2$ crystals also show (110) and ($\bar{1}\bar{1}$0) faces.

Detailed structure analyses have been made for the PF_6^- salt and for the isomorphous BF_4^- and ClO_4^- salts, the latter at 200 K (*Figs. 1–4*). In all three structures, the TMET molecules are distinctly nonplanar, being bent along their long direction into an S-shape. All the six-membered rings have the same conformation: five atoms approximately in a plane and one methin C-atom out of this plane. The Me substituents are pseudo-equatorial. The same type of S-shaped deformation, although not nearly so pronounced, can

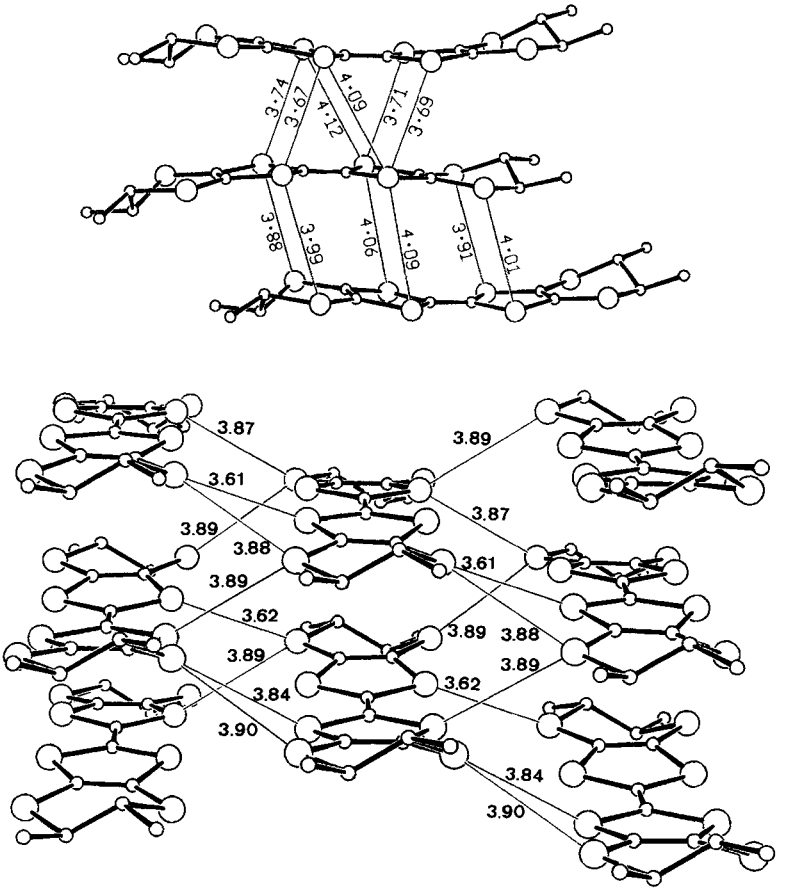

Fig. 1. *$(TMET)_2PF_6$. Short intrastack* (above) *and interstack* (below) *S···S contacts.* E.s.d.'s range from 0.007 to 0.009 Å.

be detected in several ET salts [6], and the same conformation of the six-membered ring is also seen in both series.

Both the 2:1 and 3:2 structural types contain slipped stacks of TMET molecules showing two types of overlap (A and B in *Fig. 4*). The stacking motif is ABAB... in the 2:1 type and AABAAB... in the 3:2 type (*Figs. 1* and *2*, upper parts). In both types of structure, the anions occupy channels running parallel to the *a* axis (*Fig. 3*). The walls of

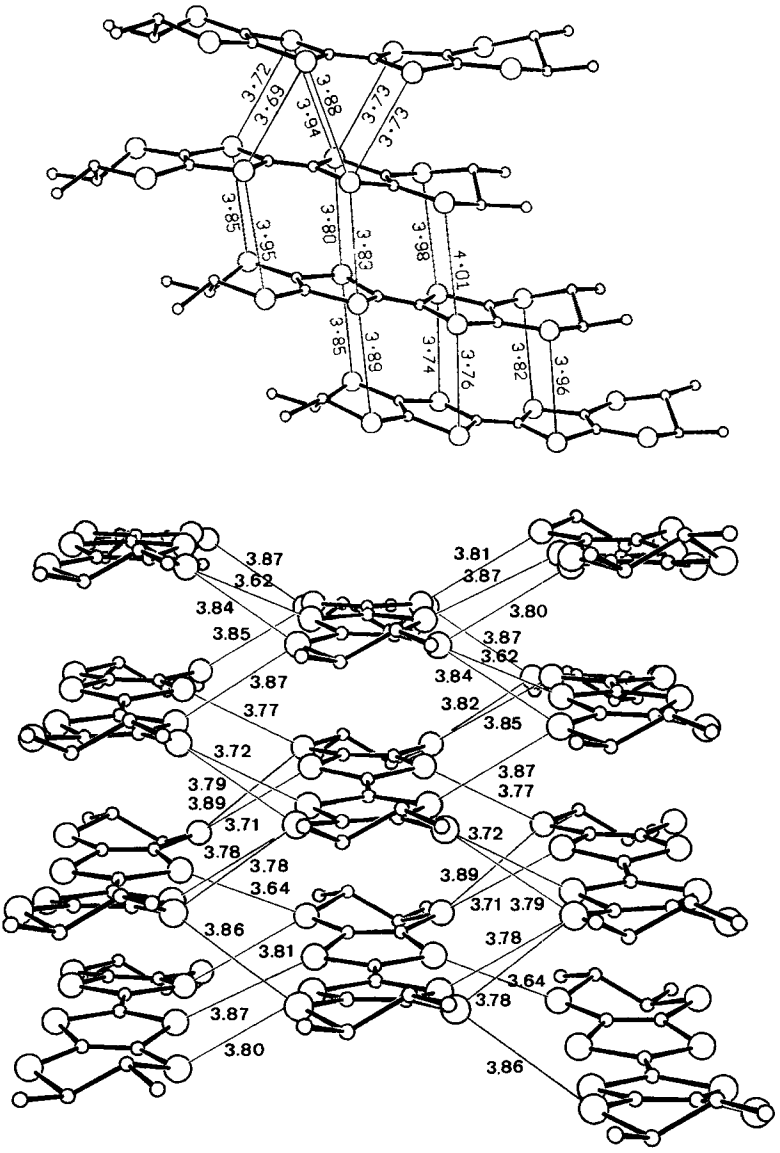

Fig. 2. *(TMET)$_3$(ClO$_4$)$_2$. Short intrastack* (above) *and interstack* (below) *S···S contacts.* E.s.d.'s range from 0.012 to 0.024 Å.

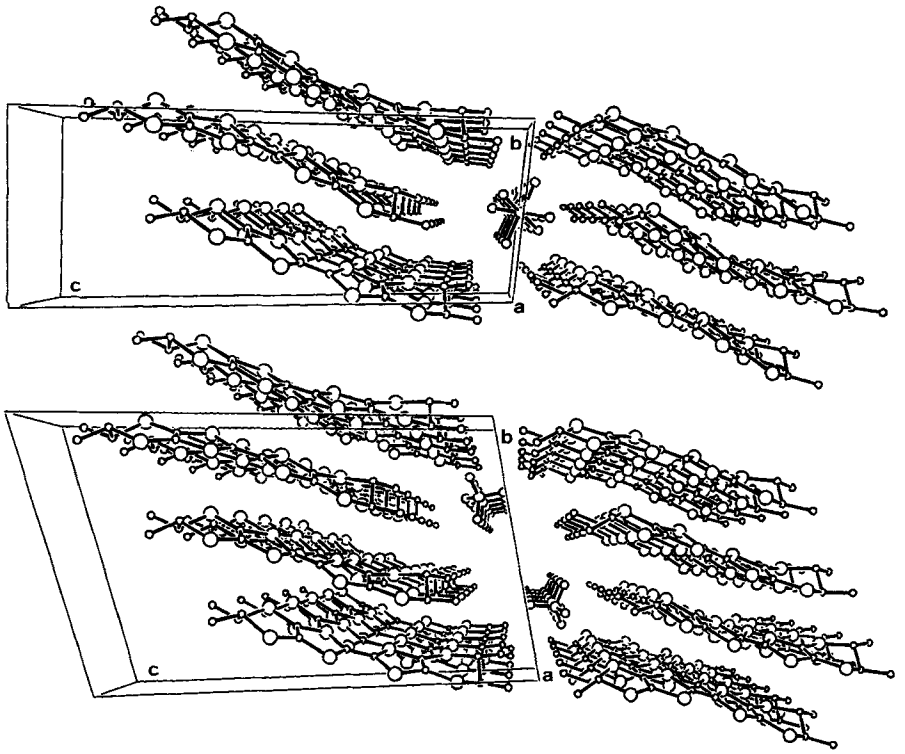

Fig. 3. *Anion channels in* $(TMET)_2PF_6$ *(above) and* $(TMET)_3(ClO_4)_2$ (below). Only one orientation of the disordered anions is shown in each picture.

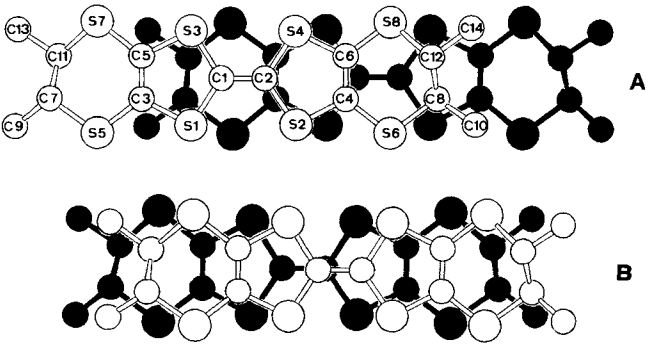

Fig. 4. *Molecular overlap observed in* $(TMET)_nX$ *structures.* The numbering scheme of the TMET molecule is shown.

these channels are made from the peripheral Me groups of surrounding TMET molecules; there are no cages in these channels, in contrast to the channels observed generally in the ET conductors. In the PF_6^- structure, the anions are distributed over two orientations; in the BF_4^- and ClO_4^- structures they are, in addition, distributed over at least two sites. Notice that, owing to the absence of inversion centers or other symmetry elements in

these structures, the anion disorder referred to here may involve translational disorder in addition to the usual kind of orientational disorder characteristic of many tetramethyltetraselenafulvalene (TMTSF) [7] and ET salts. Because of the anion disorder, it is difficult to determine the exact stoichiometry from the diffraction analyses, but it is close to 2:1 for the PF_6^- structure. In the 3:2 structures, the anion channels are larger; they could accommodate two BF_4^- (ClO_4^-) anions per unit cell, but it is also possible that neighbouring vacant sites are occupied by solvent molecules. This would explain the presence of $CHCl_3$ and $PhNO_2$ in crystals grown from these solvents (see below).

Whereas in most highly conducting ET compounds the interstack S···S contacts are shorter than the intrastack ones, there is no marked difference in the TMET salts (*Figs. 1* and *2*).

Of the two isostructural BF_4^- and ClO_4^- TMET salts, the one with the smaller anion (BF_4^-) has a larger unit cell – in contrast to the TMTSF [8] series. This is not easily explained as an influence of disorder, since the isotropic displacement factor of ClO_4^- is actually larger than that of BF_4^-. However, the anion population factors may possibly be lower in the ClO_4^- structure.

Although no detailed structure analysis has been made for the AsF_6^-, SbF_6^-, ReO_4^- and I_3^- salts (*Table 1*), precession photographs indicate that the first two are isostructural with the PF_6^- salt, while the ReO_4^- salt belongs to the BF_4^- and ClO_4^- type. The diffraction pattern of crystals grown from solutions containing I_3^- as anion shows that the arrangement of TMET molecules is quite similar to that in the PF_6^- structure, but the X-ray photographs show diffuse sheets of intensity perpendicular to [100]. This feature indicates that I-atom positions in different anion channels must be completely uncorrelated with one another. From the inter-sheet separation, which is incommensurate with a^*, the average I···I distance within a channel can be estimated to be 3.2 Å, a value often observed in other incommensurate structures containing I chains [9]. Accepted values of 3.89 Å for I···I and 2.92 Å for I–I-distances in I_3^--chain compounds also average to 3.23 Å [10]. Therefore we infer that I_3^- anions are present in the structure and estimate the composition to be $(TMET)_2(I_3)_{0.71}$.

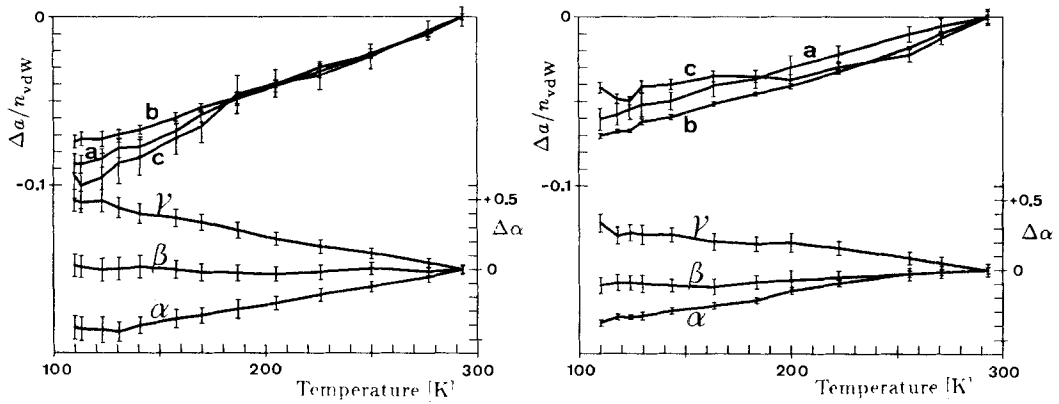

Fig. 5. *Temperature dependence of the cell constants in* $(TMET)_2PF_6$ (left) *and* $(TMET)_3(ClO_4)_2$ (right)

Although the $(TMET)_nX$ crystals were grown from a range of solvents and under a variety of experimental conditions (see *Exper. Part*), no polymorphs have been observed so far – in contrast to the $(ET)_nX$ salts, where polymorphism is almost the rule.

Fig. 5 shows the temperature dependence of the cell constants of $(TMET)_2PF_6$ and $(TMET)_3(ClO_4)_2$. We assume that the shrinkage of the molecules is negligible compared with the decrease of the intermolecular distances. The decrease in cell constant Δa, divided by n_{vdW}, the number of intermolecular contacts per unit cell in that direction, gives a kind of 'normalized' cell shrinkage; the slope of $\Delta a/n_{vdW}$ against temperature should be the same for all directions a in an ideal *van der Waals* crystal. For the a, b, and c directions, n_{vdW} is roughly 1, 2, and 1.5 in $(TMET)_2PF_6$ and 1, 3, and 1.66 in $(TMET)_3(ClO_4)_2$, respectively. The PF_6^- structure shows quite linear shrinkage in all three directions. Furthermore, the $\Delta a/n_{vdW}\Delta T$ slopes are roughly the same and thus suggest that the unit-cell shrinkage is mainly of the *van der Waals* type. The ClO_4^- compound shows similar behavior for the a and b axes, but $\Delta c/\Delta T$ has discontinuities at 200 K and also around 120 K, where a metal-insulator transition occurs. We tried to measure the crystal structure at 100 K. However, reflections that were sharp ($\Delta\theta < 1°$) after slow cooling (0.5 K/min), broadened to $\Delta\theta > 3°$ during data collection. Slow warming partially restored the original quality of the reflections.

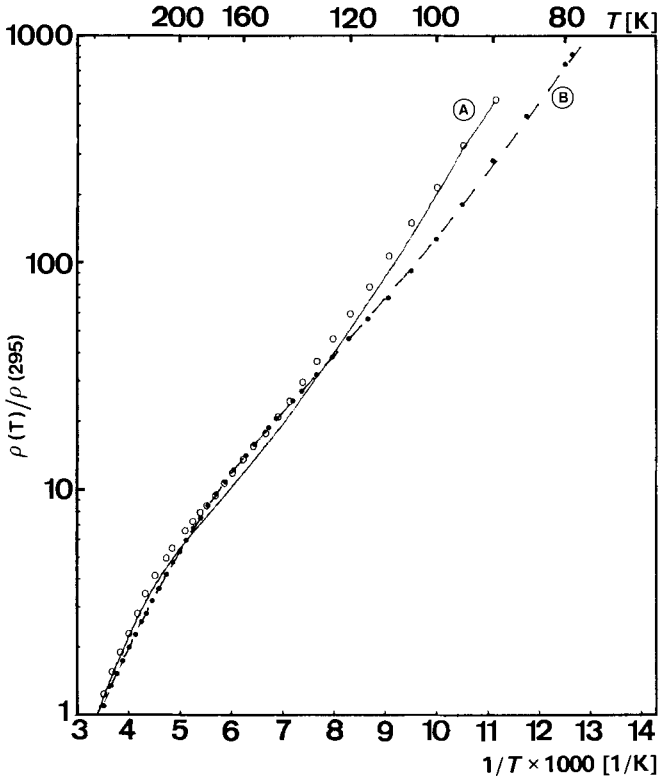

Fig. 6. *Electrical resistivity of* $(TMET)_2PF_6$, *normalized to the value at room temperature. A*, normal pressure, —— cooling, ○○○ heating; *B*, 8 kbar, – – – cooling, ●●● heating.

Electrical Properties. – The 2:1 salts $(TMET)_2X$ ($X = PF_6^-$, AsF_6^-, SbF_6^-) show semiconducting behavior along all three crystallographic directions. The room-temperature resistivity of the compounds is about 0.2 Ωcm in the *b* (stacking) direction. The resistivity ratios are approximately $\rho_a:\rho_b:\rho_c \approx 15:1:500$. $(TMET)_2(I_3)_{0.71}$ is weakly metallic down to 230 K and shows a somewhat lower room-temperature resistivity, $\rho = 8 \cdot 10^{-2}$ Ωcm. Surprisingly, none of these compounds could be made metallic by applying hydrostatic pressure up to 8 kbar. The energy gap, which is about 130 meV, does not change significantly with pressure (*Fig. 6*). A weak hysteresis, depending on the solvent used in the electrocrystallisation, shows up at normal pressure, but disappears completely under pressure. From the behavior of $d(\log\rho)/d(1/T)$ as function of T (*Fig. 7*) for the three

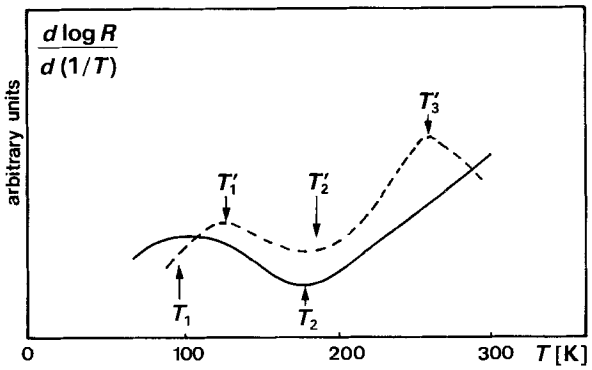

Fig. 7. *Schematic representation of possible phase transitions of the 2:1 type salts as observed by electrical resistivity measurements.* —— at normal pressure, – – – at 8 kbar.

semiconducting salts, we can detect two phase transitions at normal pressure and at least three at higher pressure (*Table 2*). Attempts to convert these semiconducting salts to a metallic state by applying pressures higher than 8 kbar are under way.

Table 2. *Transition Temperatures of 2:1 Type Salts Corresponding to* Fig. 7

		X in $(TMET)_2X$		
		PF_6^-	AsF_6^-	SbF_6^-
at normal pressure	T_1 [K]	100	135	145
	T_2 [K]	175	210	215
at p = 8 kbar	T'_1 [K]	80		100
	T'_2 [K]	135	138	125
	T'_3 [K]	265	275	240

The 3:2 salts $(TMET)_3X_2$ ($X = BF_4^-$, ClO_4^-, ReO_4^-) show metallic behavior of the resistivity in the *a* and *b* directions. So far, only $(TMET)_3(ClO_4)_2$ has been examined extensively. Its room-temperature resistivity is $\rho = 8 \cdot 10^{-2}$ Ωcm in the *b* direction and the anisotropy ratios are about $\rho_a:\rho_b:\rho_c \approx 300:1:1000$. A more detailed description is not possible at this stage because of various complications. In *Fig. 8*, the experimental results

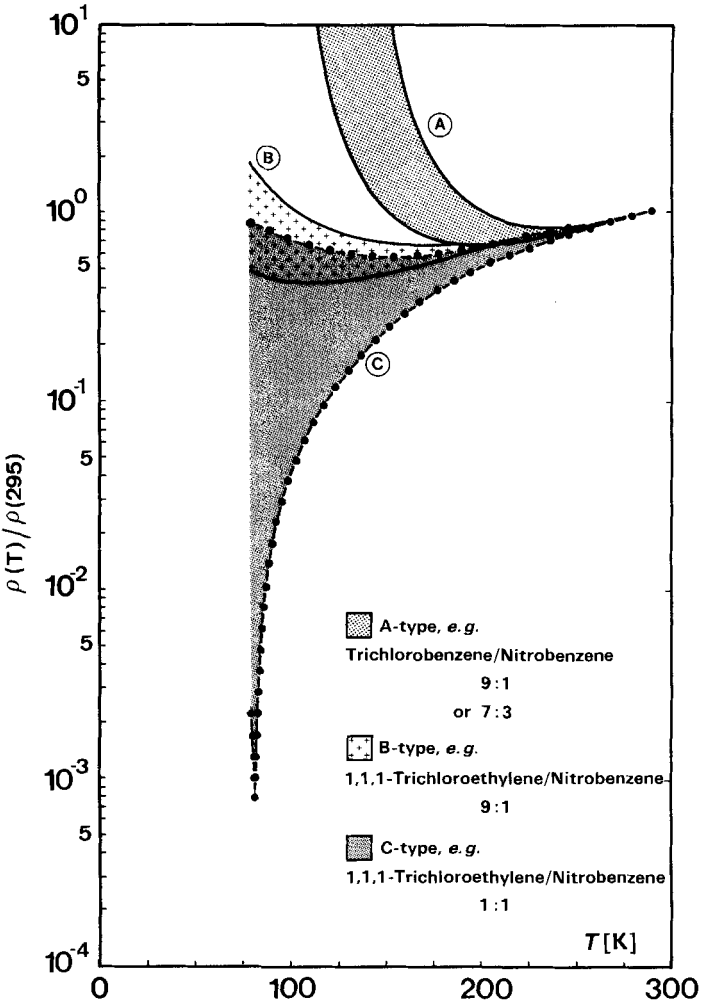

Fig. 8. *Schematic representation of ranges of different types of electrical resistivity behavior as function of temperature (normalized to the value at room temperature) for* $(TMET)_3(ClO_4)_2$ *crystals grown in various solvents*

are classified into three main types of behavior. The temperature behavior of the resistivity seems to depend on several factors, depending on the solvent used in the electrocrystallisation. Indeed, the actual presence of solvent in the crystals was unambiguously detected (MS, DSC, thermal gravimetry; up to 5% by weight), although no differences in the X-ray diffraction patterns from crystals grown from different solvents could be observed. We therefore assume that the solvent molecules must be located in the anion channels (*Fig. 3*). Although not proven, this is compatible with the available structure evidence, if exact 3:2 stoichiometry is abandoned. The presence of solvent molecules in the anion channels must have profound influence on ordering processes and hence on the temperature dependence of the resistivity.

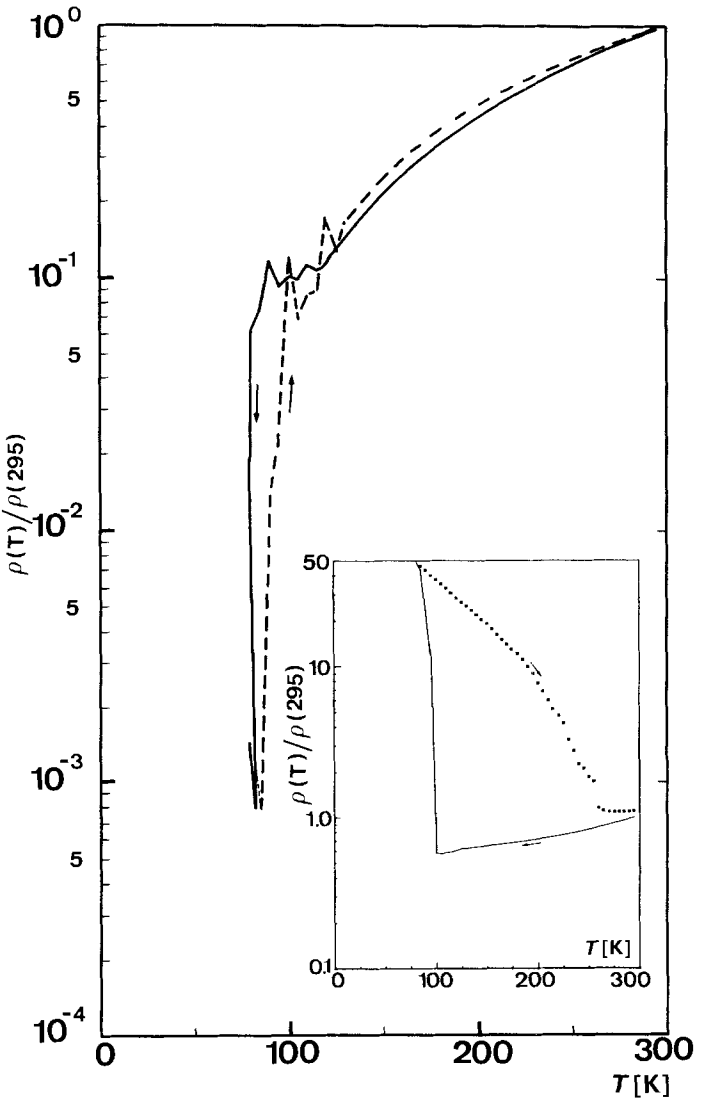

Fig. 9. *Electrical resistivity (normalized to the value at room temperature) of a C-type* $(TMET)_3(ClO_4)_2$ *crystal* (see *Fig. 8*). —— cooling, – – – heating. Insert: Electrical resistivity of a B-type crystal, showing large hysteresis.

In C-type batches only about one crystal in four shows a dependence similar to that depicted in *Fig. 9*. Such crystals show a much smaller hysteresis than those with smooth metallic behavior (compare with insert in *Fig. 9*). On repeated heating and cooling of a given crystal, its behavior can change. The temperature dependence of the resistivity when measured under pressure is shown in *Fig. 10*. The pressure of the clamp cell was 8 kbar. Crystals grown from different solvents show different behavior, but also crystals from the same batch sometimes behave differently (compare curves *4* and *5* in *Fig. 10*). Note that for sample *5* the metallic state is stable down to 2 K.

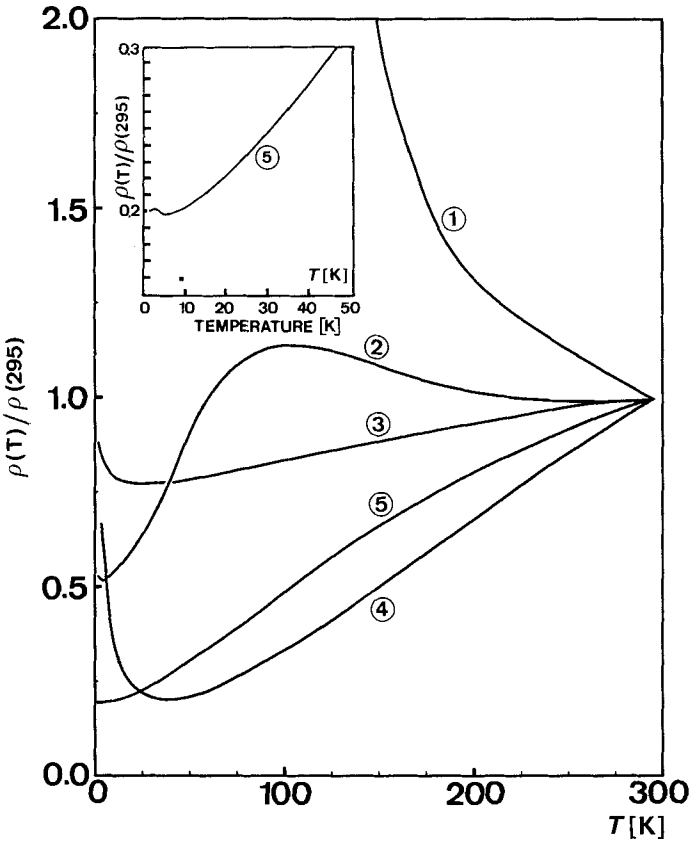

Fig. 10. *Electrical resistivity of* $(TMET)_3(ClO_4)_2$ *crystals (normalized to the value at room temperature) under 8 kbar hydrostatic pressure.* Crystals were grown in: ①, CH_2Cl_2; ②, 7:3 mixture of 1,2,4-trichlorobenzene/$PhNO_2$; ③, 7:3 mixture of 1,1,1-trichloroethane/$PhNO_2$; ④ and ⑤ 1:1 mixture of 1,1,1-trichloroethane/$PhNO_2$. Insert: Low-temperature part of *5*.

Conclusions. – Individual crystal specimens grown from the same solvents can show widely different electrical behavior, especially in the temperature dependence. These differences are probably caused by different amounts, proportions, and distributions of solvent molecules and anions in the anion channels. The lack of a method to control or measure these parameters has seriously hampered our attempts to systematize and understand the electrical properties and structural findings more deeply.

Some features of the crystallographic investigations (the haloes evident on *Weissenberg* photographs, large anisotropic displacement parameters, residual disorder, uninterpretable residual electron density, time-dependent reflection-broadening over periods of several days at 100 K) of $(TMET)_3(ClO_4)_2$ make us believe that some high-order phase transition (anion ordering? incommensurate phase?) occurs at *ca.* 120 K, where also an electronic phase transition is observed. We envisage that a slow structure change of this type might be attributable to an anion ordering rather than to a *Peierls*-type transition.

Experimental Part

Preparation. – The synthesis of TMET has already been described [5]. Crystals of the 2:1 type were grown with practically identical results from sat. TMET solns. in either $CHCl_3$ or in a 7:3 mixture of 1,1,1-trichlorethane and $PhNO_2$. The concentration of the supporting tetrabutylammonium electrolyte salts was of the order of 0.1 mol/l for all experiments. Typical growing currents for the electrocrystallisation at r.t. were 0.5 μA with Pt wire electrodes (1 × 20 mm). The current was gradually increased to its final value over 3 days, and crystal growth continued over 3 weeks. Typical dimensions of the resulting crystals are 3 × 2 × 0.2 mm^3 for platelets and 5 × 1 × 0.2 mm^3 for needles. Crystals of the 3:2 type were more difficult to grow because of the rather high solubility of the product salts. The same electrolyte concentration and growing currents were used in this series as for the 2:1 type compounds. So far, the most satisfying results (*Fig. 9*) were obtained with a 1:1 mixture of 1,1,2-trichlorethane and $PhNO_2$, with the electrolysis cell held at 0°. Crystals have also been grown in $CHCl_3$, CH_2Cl_2, and 1,1,1-trichlorethane; optimizations are in progress.

Electrical Measurements. – Four-probe electrical resistivity measurements were made using direct current. The Au wires used were 15 μm thick and attached to the crystals with Pt-paste *Degussa 308*. For the electrical resistivity measurements at high pressure, only needle-shaped crystals have been used so far. The crystal holder was positioned in a Be-Cu high-pressure clamp cell so that the needle axis (*b*) was parallel to the cell axis. As pressure transmitting medium, we used silicon oil *Merck* type *350*. The starting pressure was 8.1 kbar.

Crystallographic Studies. – *General. Enraf Nonius CAD4* automated four-circle diffractometer, low-temp. device, graphite-monochromated Mo$K\alpha$ radiation (λ = 0.71069 Å). Unit-cell dimensions from least-squares refinement of the setting angles of 12 reflections ($8° < \theta < 12°$), ω-scan, variable scan rate (30...80 sec per reflection). *Lorentz*-polarisation correction, no absorption correction. Standard atomic scattering factors (anomalous for S, P, and Cl) were used [11]. Further crystallographic data are given in *Table 3*. Because of the nearly centrosymmetric

Table 3. *Crystal Data for Three TMET Salts*

Compound	$(TMET)_2PF_6$	$(TMET)_3(ClO_4)_2$	$(TMET)_3(BF_4)_2$
Temperature	298 K	200 K	298 K
Space group	$P\bar{1}$	$P\bar{1}$	$P\bar{1}$
$\sin\theta/\lambda$ limit	0.595	0.550	0.550
Reflections measured	3596	4921	4496
Reflections used ($F_o > 6\sigma(F_o)$)	2271	3638	2662
Parameters refined	305	432	432
Final R value	0.049	0.133	0.079

arrangement of the anomalous scatterers, no *Bijvoet* effect could be detected, and no absolute structure determination was attempted. Application of SHELX-86 [12] in space group $P\bar{1}$ revealed the central part of the TMET molecules. Remaining non-H-atoms were located using *Fourier* methods (SHELX-76 [13]), and the reduction of the space-group symmetry to $P\bar{1}$ was effected by choosing the positions of the Me C-atoms to give the same configuration (*S*) to all asymmetric C-atoms. Full-matrix least-squares refinement in space group $P\bar{1}$ suffered from severe correlations of parameters related by the pseudo-inversion center, preserving the overall structure but introducing unreasonable bond lengths. By constraining chemically equivalent bonds to have the same length, the correlations became manageable: the S-atoms could be refined anisotropically. For the inner C-atoms of the TMET molecules (C(1)...C(6)), the coordinates are still doubtful. The anions were constrained to have appropriate symmetry; a single isotropic atomic displacement parameter was used for all F- (or O-) atoms.

$(TMET)_2PF_6$. The PF_6^- anion was found to occupy two preferred orientations, each with an occupancy factor of 0.5. Only one orientation is shown in the *Figures*.

$(TMET)_3(ClO_4)_2$. Fourier methods failed here to establish the positions of the terminal methin and Me C-atoms unambiguously. Since it was suspected that the six-membered rings had the same conformation as in the PF_6^- structure and in the TMET monomer [14], each TMET molecule could be modeled leaving an uncertainty about which of the two methin C-atoms per six-membered ring was out-of-plane. From the internal molecular coordinates of the TMET monomer structure, each of the 64 possible permutations was generated, and a structure factor calculation was performed. The solution with the lowest R factor was then subjected to the constrained

least-squares refinement (S anisotropic, H-atoms omitted) which converged to $R = 0.133$. Residual electron density maxima of 1.18 $e\text{Å}^{-3}$ in the anion channel region indicate that there is severe anion disorder in this crystal.

(TMET)$_3$(BF$_4$)$_2$. The structure was solved by using the coordinates of the isostructural ClO_4^- compound. Illustrations for $(TMET)_3(ClO_4)_2$ are also valid for $(TMET)_3(BF_4)_2$.

We thank Dr. *P. Kriemler* for recording the MS spectra, Dr. *E. Marti* and *E. Minder* for the thermal analysis, and *M. Rudin* for technical assistance in the electrical measurements. This work was partly supported by the *Swiss National Science Foundation*.

REFERENCES

[1] S.S.P. Parkin, E.M. Engler, R.R. Schumaker, R. Lagier, V.Y. Lee, J. Voiron, K. Carneiro, J.C. Scott, R.L. Greene, *J. Phys. (Paris) Colloq., Suppl.* **1983,** *44,* C3–791; G. Saito, T. Enoki, H. Inokuchi, H. Kobayashi, *ibid.* **1983,** *44,* C3–1215.

[2] E.B. Yagubskii, I.F. Shegolev, V.N. Laukhin, P.A. Kononovich, M.W. Karatsovnik, A.V. Zvarykina, L.I. Buravov, *Pis'ma Zh. Eksp. Teor. Fiz.* **1984,** *39,* 12; *JETP Lett. (Engl. Transl.)* **1984,** *39,* 12.

[3] M. Tokumotu, K. Murata, H. Bando, H. Anzai, G. Saito, K. Kajimura, T. Ishoguro, *Solid State Commun.* **1985,** *54,* 1031.

[4] H.H. Wang, M.A. Beno, U. Geiser, M.A. Firestone, K.S. Webb, L. Nuñez, G.W. Crabtree, K.D. Carlson, J.M. Williams, L.J. Azevedo, J.F. Kwak, J.E. Schirber, *Inorg. Chem.* **1985,** *24,* 2466; E. Amberger, K. Polborn, H. Fuchs, *Angew. Chem.* **1986,** *98,* 749; *ibid. Int. Ed.* **1986,** *98,* 727; E. Amberger, H. Fuchs, K. Polborn, *Angew. Chem.* **1986,** *98,* 751; *ibid. Int. Ed.* **1986,** *98,* 729; H. Endres, M. Hiller, H.J. Keller, K. Bender, E. Gogu, I. Heinen, D. Schweitzer, *Z. Naturforsch., B* **1985,** *40,* 1664; H. Kobayashi, M. Takahashi, R. Saito, A. Kobayashi, Y. Sasaki, *Chem. Lett.* **1984,** 1331.

[5] J.D. Wallis, A. Karrer, J.D. Dunitz, *Helv. Chim. Acta* **1986,** *69,* 69.

[6] R.P. Shibaeva, V.F. Kaminskii, E.B. Yagubskii, *Mol. Cryst. Liq. Cryst.* **1985,** *119,* 361; P.C.W. Leung, M.A. Beno, G.S. Blackman, B.R. Coughlin, C.A. Miderski, W. Joss, G.W. Crabtree, J.M. Williams, *Acta Crystallogr., Sect. C* **1984,** *40,* 1331.

[7] J.P. Pouget, G. Shirane, K. Bechgaard, J.M. Fabre, *Phys. Rev. B* **1983,** *27,* 5203.

[8] T.J. Kistenmacher, *Mol. Cryst. Liq. Cryst.* **1986,** *136,* 361.

[9] A. Filhol, J. Gaultier, C. Hauw, B. Hilti, C.W. Mayer, *Acta Crystallogr., Sect. B* **1982,** *38,* 2577.

[10] F.H. Herbstein, M. Kaftory, M. Kapon, W. Saenger, *Z. Kristallogr.* **1981,** *154,* 11.

[11] International Tables for X-Ray Crystallography, Vol. IV, Kynoch Press, Birmingham, England, 1974.

[12] G.M. Sheldrick, in 'Crystallographic Computing 3', Eds. G.M. Sheldrick, C. Krüger, and R. Goddard, Oxford University Press, Oxford, 1985, p. 175.

[13] G.M. Sheldrick, 'SHELX76, a Program for Crystal Structure Determination', University of Cambridge, England, 1976.

[14] J.D. Wallis, J.D. Dunitz, to be published in *Acta Crystallogr.*